Available online at www.sciencedirect.com
SCIENCE DIRECT®
Journal of Nuclear Materials 326 (2004) 30–37
journal of nuclear materials
www.elsevier.com/locate/jnucmat

Irradiation damage in 304 and 316 stainless steels: experimental investigation and modeling. Part II: Irradiation induced hardening

C. Pokor [a,b], Y. Brechet [c], P. Dubuisson [a], J.-P. Massoud [d,*], X. Averty [e]

[a] CEA/DEN/SRMA, CEA Saclay, 91191 Gif sur Yvette cedex, France
[b] EDF/GDL/SECH, BP23-37420 Avoine cedex, France
[c] LTPCM, BP75, Domaine Universitaire de Grenoble, 38402 Saint Martin d'Heres cedex, France
[d] EDF R&D–MMC–Site des Renardières, 77818 Moret sur Loing cedex, France
[e] CEA/DEN/SEMI, CEA Saclay, 91191 Gif sur Yvette cedex, France

Received 6 December 2003; accepted 15 December 2003

Abstract

The consequences of irradiation damage in austenitic stainless steels on their mechanical properties, namely the yield stress, are investigated both experimentally and theoretically. The observed hardening is correlated with the quantitative characteristics of irradiation defects population. A simple model allowing for the defaulting of Frank loops under stress predicts the hardening and its saturation at large doses.

PACS: 61.80; 61.72.F; 81.40.C,E; 62.20.F

1. Introduction

In the companion paper [1], a systematic quantitative characterization of irradiation induced microstructures in 304L, 316 and 316 Ti austenitic stainless steels has been performed on samples irradiated under different conditions: flux, dose, energy spectra (fast and mixed spectrum) and irradiation temperature (330 and 375 °C). These results have been modeled using a cluster dynamics approach specially adapted to account for the evolution of the point defects created by irradiation and for the formation of a Frank loop dislocation substructure.

As a result of this microstructural evolution under irradiation, these materials undergo a substantial increase in yield stress and reduction in ductility. In the present contribution, we will focus our attention only on the consequences of this microstructural evolution on the yield stress. We will assume that the hardening is mainly due to the population of Frank loops, as irradiation induced precipitation (e.g. γ'), which could contribute to irradiation hardening, was not observed in our specimens. This hardening depends both on the initial metallurgical state of the alloy and on the irradiation conditions. Of special interest will also be the question of the possible saturation of microstructural evolution and related hardening for long term irradiation.

The aim of this paper is to provide a quantitative measurement of the evolution of the mechanical properties (yield stress) by post-irradiation tensile tests at constant strain rate. The modeling of the evolution of yield stress for a given microstructure will be proposed using classical dislocation theory. The parameters entering this model will be identified from the experimental tensile curves, and the prediction of the model will be compared with experiments for larger doses.

* Corresponding author. Address: EDF R&D–MMC–Site des Renardières, 77818 Moret sur Loing cedex, France. Tel.: +33-1 60 737105; fax: +33-1 60 736889.
E-mail address: jean-paul.massoud@edf.fr (J.-P. Massoud).

0022-3115/$ - see front matter
doi:10.1016/j.jnucmat.2003.12.008

The materials investigated and the irradiation conditions have already been reported in companion paper I; they will not be recalled in this paper. In Section 1, we outline the proposed mechanism for the evolution of yield stress, and give a brief summary of the findings of paper I. Section 2 presents the experimental conditions for tensile testing and the measured yield stresses for the different alloys and irradiation conditions. In Section 3 we propose a model for the yield stress evolution coupling the hardening by dislocation loops and the question of their stability. The predictions of this model are finally compared with the experimental results.

2. Testing conditions and experimental results

2.1. Tensile testing method

Small cylindrical specimens with a gauge length of 12 mm and a diameter of 2 mm were machined from the three investigated materials: solution annealed SA 304L, CW 316 and CW Ti-modified 316 stainless steels (Fig. 1).

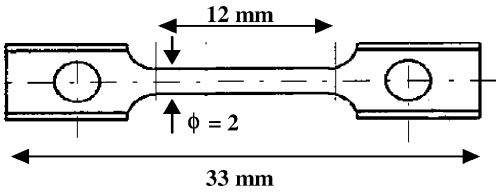

Fig. 1. Cylindrical tensile test specimens irradiated in the different reactors.

For the SA 304L plate, specimens were cut and machined perpendicularly to the rolling direction at mid-thickness of the plate. For the CW 316 bars, specimens were sampled along the drawing direction, at about mid-radius of the rod.

These specimens were irradiated in different experimental reactors (BOR-60, Dimitrovgrad, Russia; Osiris, Saclay, France, and EBRII, USA) as detailed in paper I.

The tensile tests were performed both on unirradiated and irradiated specimens in hot cells at the RIAR (Dimitrovgrad) for materials irradiated in BOR-60 and in hot cells at the CEA (Saclay) for materials irradiated in Osiris and EBR II. The tests were performed at a conventional strain rate of 3×10^{-4} s^{-1} and at the same temperature as the irradiation temperature (i.e. at 330 °C for materials irradiated in BOR-60 and Osiris and at 375 °C for the materials irradiated in EBR II). Tests are led in an electric resistance furnace. Repeat tensile tests were carried out both at the RIAR and the CEA confirming that both hot-laboratories produce comparable and coherent results.

After the tests, the conventional parameters (in particular the conventional yield stress at 0.2% plastic strain) are estimated from the tensile curve.

2.2. Engineering tensile curves

Examples of engineering tensile curves for SA 304L and CW 316 irradiated at about 20 dpa are reported in Fig. 2. These curves are typical of austenitic steels

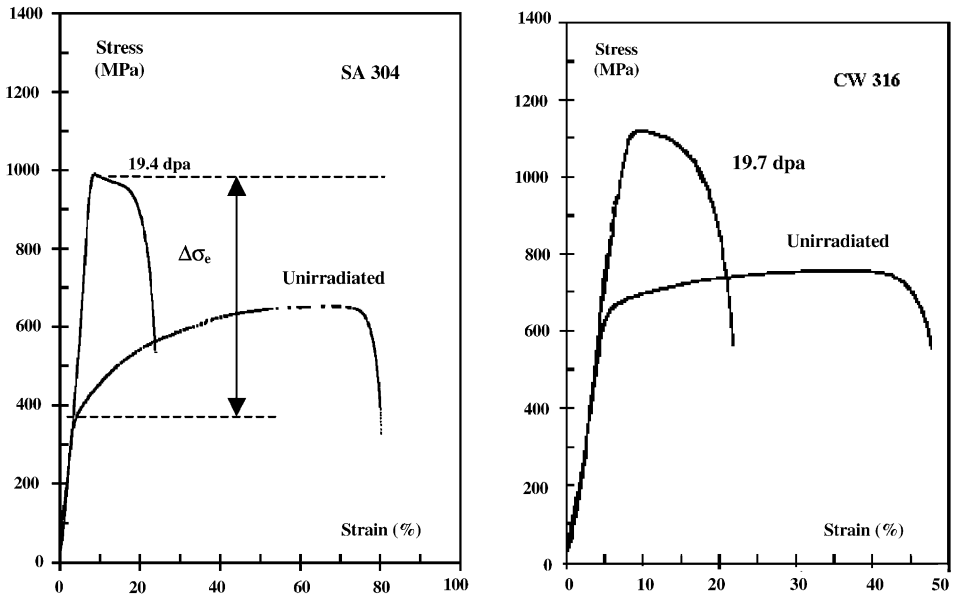

Fig. 2. Engineering stress–strain curves for the SA 304L and CW 316 steels irradiated in BOR-60 reactor.

irradiated at low temperatures and doses above the saturation dose for irradiation hardening. Large dose irradiations lead to a large increase in yield stress associated with an important loss of ductility. The yield and ultimate tensile stress are almost equal.

A model describing the evolution of the yield stress with irradiation is developed in the following sections.

2.3. Evolution of the yield stress of the irradiated materials

A measure of irradiation hardening is the difference of yield stress at 0.2% plastic strain between irradiated ($\sigma_{e,i}$) and unirradiated ($\sigma_{e,ni}$) materials: $\Delta\sigma_e = \sigma_{e,i} - \sigma_{e,ni}$. $\Delta\sigma_e$ is reported as a function of the dose in Fig. 3 for the three different steels (SA304L, CW316 and CW316 Ti) irradiated in the BOR-60, Osiris and EBR II reactors.

The magnitude of the hardening depends on the irradiation damage dose, on irradiation conditions (temperature, flux, spectrum ...) and the initial state of the materials (chemistry, state of deformation).

2.3.1. Influence of damage dose

Whatever the materials and the irradiation conditions may be, the hardening increases rapidly at low doses saturating for doses above 5 dpa. The values at saturation depend on chemical composition and initial metallurgical state. The tensile properties saturate at doses close to 5 dpa for the SA 304L steel and at a dose slightly higher (but still lower than 10 dpa) for the CW 316 steel. This is in agreement with the literature where saturation doses are found to be in the range of 5–10 dpa depending on the irradiation temperature [2].

2.3.2. Influence of neutron irradiation parameters (flux, spectrum, temperature)

All things being equal, there is no obvious effect of the neutron irradiation parameters (flux, spectrum) on irradiation hardening. As shown in Fig. 3, for equivalent doses, the hardening is similar for materials irradiated in a reactor with fast spectrum (BOR-60) and in a reactor with mixed spectrum (Osiris). For all the materials, the hardening is significantly higher after irradiation at 330 °C than after irradiation at 375 °C (BOR-60 and Osiris compared to EBR II).

2.3.3. Influence of metallurgical state

The saturation hardening is higher for the solution annealed 304 material (about 620 MPa) than for the two cold worked 316 and 316 Ti materials (about 500 MPa).

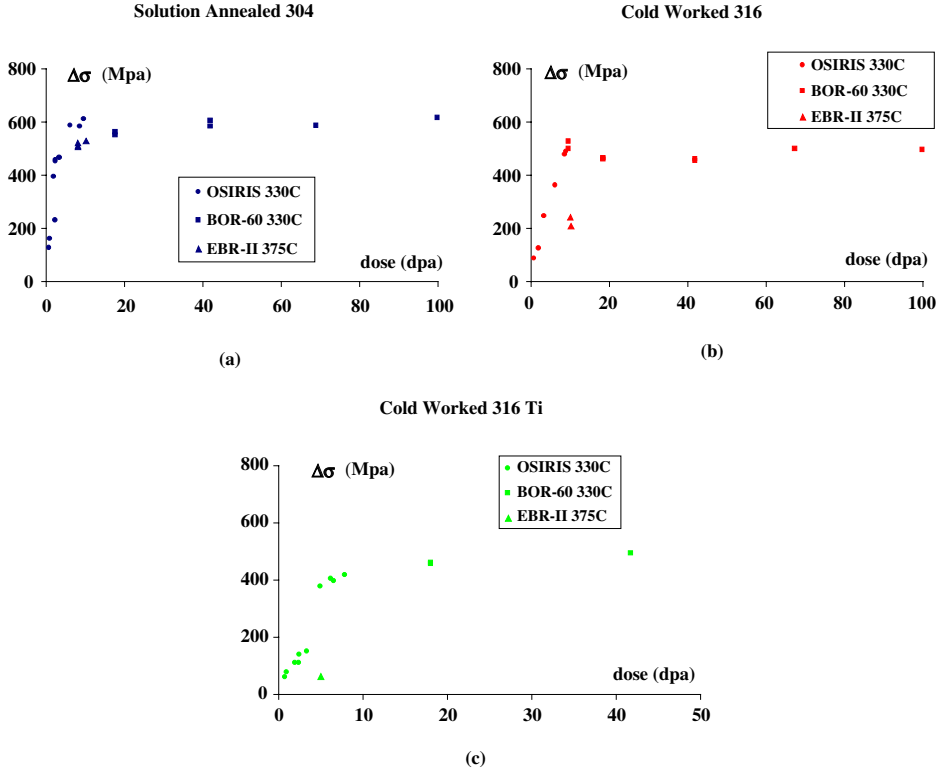

Fig. 3. Hardening for the different materials as a function of irradiation damage dose: (a) SA 304H, (b) CW 316 and (c) CW 316 Ti.

The respective influence of chemical composition and initial dislocation density on hardening cannot be definitively separated from these results. Nevertheless, we can reasonably assume that the irradiation defects dynamics is mainly dependent on the initial dislocation density (see paper I) and that a cold worked material will harden less than a solution annealed material. Chemical composition may play a role in the saturation dose for hardening: the hardening still slightly increases up to doses as high as 40 dpa for the CW 316 Ti steel, whereas there is saturation at 10 dpa for the CW 316 material.

3. Modeling the yield stress

In this section we propose a model for the yield stress evolution coupling the hardening by dislocation loops and the question of their stability, and we compare the predictions of this model with the experimental results.

3.1. Principles of the irradiation hardening model

3.1.1. Dislocation loop hardening

The principle of the modeling used here is to describe the hardening resulting from the interaction of mobile dislocations with a population of small dislocation loops induced by irradiation. The hardening is the consequence of a population of faulted Frank loops, with an average diameter ϕ_L and density ρ_L pinning the mobile dislocations. Following the classical models for irradiation hardening [3], the yield stress evolution, $\Delta\sigma = \sigma_{e,i} - \sigma_{e,ni}$ (where $\sigma_{e,i}$ designs the yield stress after irradiation and $\sigma_{e,ni}$ before irradiation) can be expressed as

$$\Delta\sigma = M\alpha_L\mu b\sqrt{\rho_L\phi_L}, \tag{1a}$$

where M is the Taylor factor, α_L the obstacle strength of the Frank loop, μ the shear modulus and b the Burgers vector. Implicit in this expression, it is assumed that the density of dislocations from the initial dislocation network is low compared to the density of Frank loops created under irradiation, and thus that its contribution to hardening is negligible. This assumption is realistic when the material is solution annealed. But when the material is cold worked, it is necessary to account for the initial dislocation network and its evolution under irradiation.

Giving ρ_0, the dislocation density of cold worked material before irradiation and ρ_d, the dislocation density remaining after a given irradiation dose, Eq. (1a) can be expressed for cold worked materials as

$$\Delta\sigma = M\mu b[\alpha_L\sqrt{\rho_L\phi_L} + \alpha\sqrt{\rho_d} - \alpha\sqrt{\rho_0}], \tag{1b}$$

where α describes the strength of obstacles created by forest dislocations [4]. The loops diameter and density

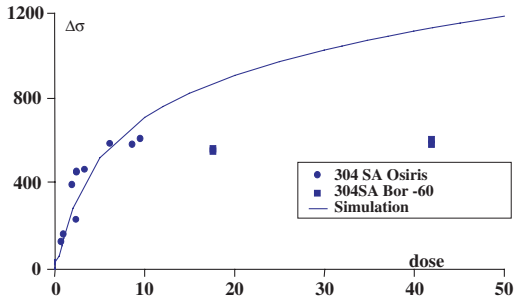

Fig. 4. Evolution of hardening as a function of irradiation damage dose for the solution annealed 304 stainless steel. The experimental data clearly show a saturation of hardening whereas the model incorporating both loop hardening and a recovery of the initial dislocation network predicts an ever increasing hardening.

are coming from the cluster dynamic model developed in the companion paper [1]. The recovery kinetics of the initial dislocation structure due to absorption of point defects and mutual annihilation of dislocations by climb is also given in the companion paper [1].

It has been shown previously [1] that the density and size of Frank loops rapidly increases up to doses of 5–10 dpa and then slightly increase for damage doses higher than 10 dpa. This suggests that irradiation hardening should not saturate with dose. This is in contradiction with experimental data; Fig. 4 clearly showing the saturation of yield stress for doses beyond 10 dpa.

It seems that although the irradiation damage increases the hardening efficiency of the Frank loops is decreasing. The missing ingredient stems from the limited stability of Frank loops for increasing applied stress. This approach is developed in the following section.

3.1.2. Influence of the instability of the faulted Frank loops

It is known that in materials with low Stacking Fault Energy (as is the case for the austenitic stainless steels of the present study), small faulted Frank loops are more stable than the perfect dislocation loops of equivalent size. The reason for this situation is that a partial dislocation has a line energy smaller than that of perfect dislocations. For small radii, this difference in line energy can pay for the cost associated with the stacking fault present in the Frank loop. For large radii, the energy of a faulted loop is higher than that of a perfect loop, meaning that above a critical radius (R^*) faulted loops tend to default to form perfect loops. Under an applied stress, the situation changes. The Peach–Koehler force does work on the partial dislocation required to default the Frank loop thus changing the energy balance and reducing the critical radius for Frank loop stability.

An estimation of the reduction in critical radius with an applied stress can be obtained from a simple energetic argument, described in the following.

Let E_F be the energy of a Frank loop with radius R and Burgers vector $b_F\left(\frac{1}{3}a\langle 1\,1\,1\rangle, b_F = a\frac{\sqrt{3}}{3}\right)$ and E_P the energy of a perfect loop with radius R and Burgers vector $b_p\left(\frac{1}{2}a\langle 1\,1\,0\rangle, b_p = a\frac{\sqrt{2}}{2}\right)$. The difference in energy between the two loops also depends on the stacking fault energy γ. When applying a shear stress τ, the work of the Peach–Kohler force acting on the partial dislocation (with Burgers vector $\sqrt{b_p^2 - b_F^2}$) alters the energy balance. The sessile Frank loop will turn into a perfect glissile loop when the stress exceeds a critical value $\tau(R)$ such as

$$E_F > E_P - \pi R^2 \tau(R)\sqrt{b_P^2 - b_F^2}. \tag{2a}$$

Expressing E_F and E_P as functions of the line and stacking fault energies, the criterion for loops to be defaulted can be expressed as

$$2\pi R\frac{\mu b_F^2}{2} + \gamma\pi R^2 > 2\pi R\frac{\mu b_p^2}{2} - \pi R^2\tau(R)\sqrt{b_p^2 - b_F^2} \tag{2b}$$

leading to a critical local shear stress $\tau^*(R)$ which must be exceeded for loops of radius R to be defaulted.

$$\tau(R) > \frac{1}{\sqrt{b_p^2 - b_F^2}R}\left\{\mu\left(b_P^2 - b_F^2\right) - \gamma R\right\} = \tau^*(R). \tag{3a}$$

Introducing the critical radius for spontaneous defaulting, the critical stress $\tau^*(R)$

$$\tau^*(R) = \frac{\gamma}{\sqrt{b_p^2 - b_F^2}}\left\{\frac{R^*}{R} - 1\right\} \tag{3b}$$

with

$$R^* = \frac{\mu(b_P^2 - b_F^2)}{\gamma}. \tag{3c}$$

The local stress required for the loops with radius R to be defaulted is thus

$$\sigma^*_{local}(R) = M\frac{\gamma}{\sqrt{b_p^2 - b_F^2}}\left\{\frac{R^*}{R} - 1\right\} \tag{3d}$$

with M being the Taylor factor.

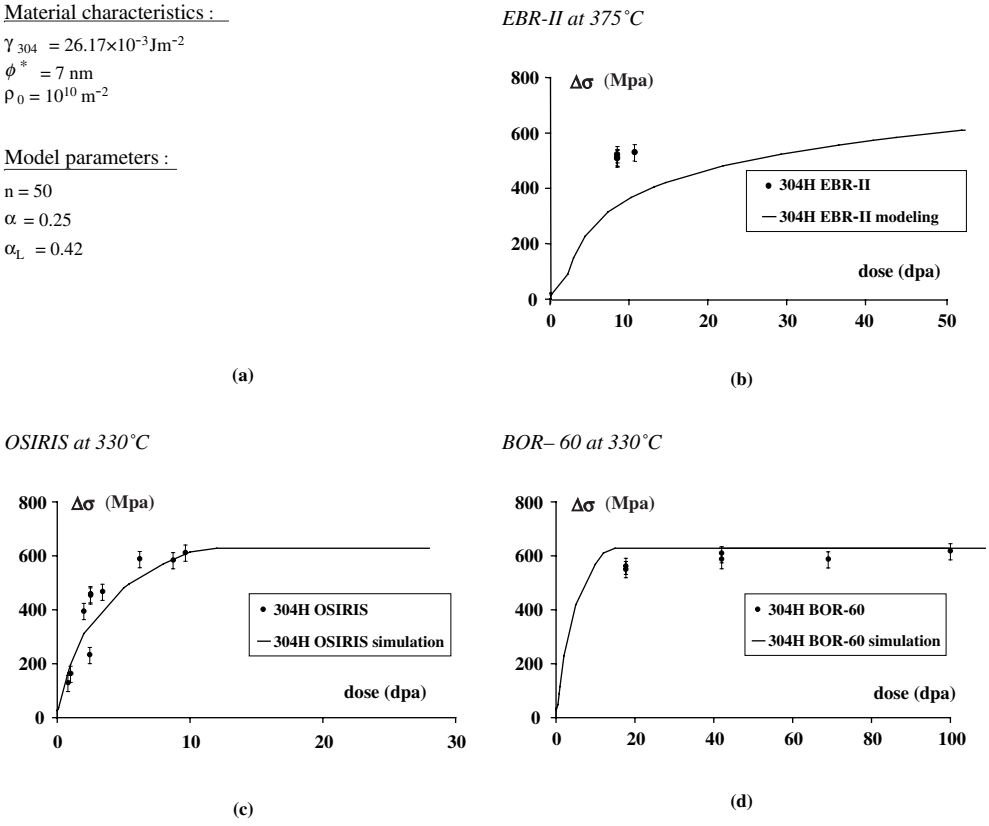

Fig. 5. Evolution of hardening for material SA 304. (a) Values of the material and model parameters, (b) EBR-II, (c) OSIRIS, (d) BOR-60.

Assuming that the local stress on Frank loops is mainly due to the pile-up of mobile dislocations, the local stress can be expressed as a function of the applied stress (σ_a) and the number of dislocations in the pile-up n. The macroscopic stress required for the loops of diameter $\phi_L = 2R$ to be defaulted can be expressed as

$$\sigma^*(\phi) = M\frac{\gamma}{n\sqrt{b_p^2 - b_F^2}}\left\{\frac{\phi^*}{\phi_L} - 1\right\}. \quad (3e)$$

The number of dislocation n in the pile-up is the only adjustable parameter not experimentally measured. In principle it could be evaluated by measuring the steps size on grain boundaries during in situ deformation [5].

When irradiation dose increases ρ_L and ϕ_L both increase and the stress required to plastically deform the material increases up to a point where stress induced defaulting of Frank loops takes place. After being defaulted, the Frank loops will turn into glissile perfect loops susceptible to move along the dislocation line and to be easily eliminated [6,7]. When a sufficient number of loops is defaulted, the stress to plastically deform the material drops below the critical value given by Eq. (3e).

Assuming that the hardening is mainly due to the Frank loops, combining Eqs. (1a) and (3e) leads to the following expression for the maximum density $\rho^*(\phi_L)$ of Frank loops of a given diameter.

$$M\alpha_L\mu b\sqrt{\rho^*(\phi_L)\phi_L} \geqslant M\frac{\gamma}{n\sqrt{b_p^2 - b_F^2}}\left\{\frac{\phi^*}{\phi_L} - 1\right\}. \quad (4a)$$

Since ρ^* is a decreasing function of ϕ_L, the opposite variation with dose is responsible for the apparent saturation. The corresponding hardening is given by

$$\Delta\sigma^* = M\alpha_L\mu b\sqrt{\rho^*(\phi_L)\phi_L} = M\frac{(\phi^* - \phi_L)}{\phi_L}\left(\frac{\gamma}{n\sqrt{b_p^2 - b_F^2}}\right) \quad (4b)$$

with $\phi^* = 2\frac{\mu(b_P^2 - b_F^2)}{\gamma}$.

3.2. Parameter identification and predictions

The model described above involves a number of parameters. The parameters related to the crystallography are the following: $a = 3.598 \times 10^{-10}$ m, then

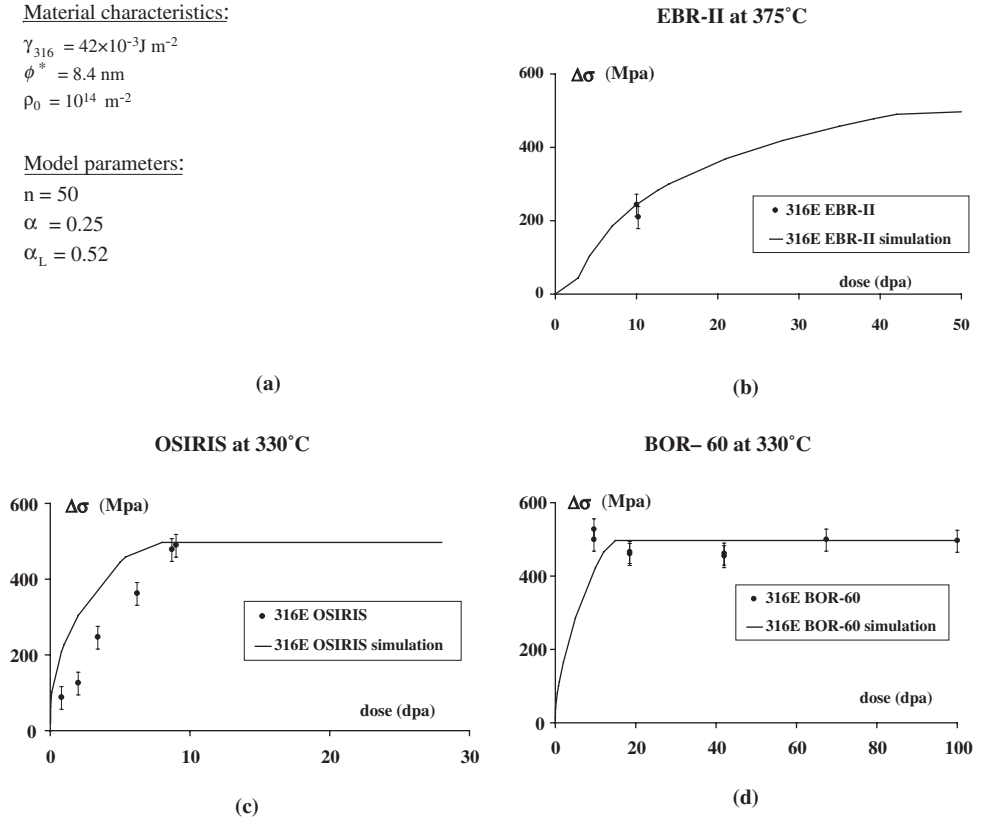

Fig. 6. Evolution of hardening for material CW 316. (a) Values of material and model parameters, (b) EBR-II, (c) OSIRIS, (d) BOR-60.

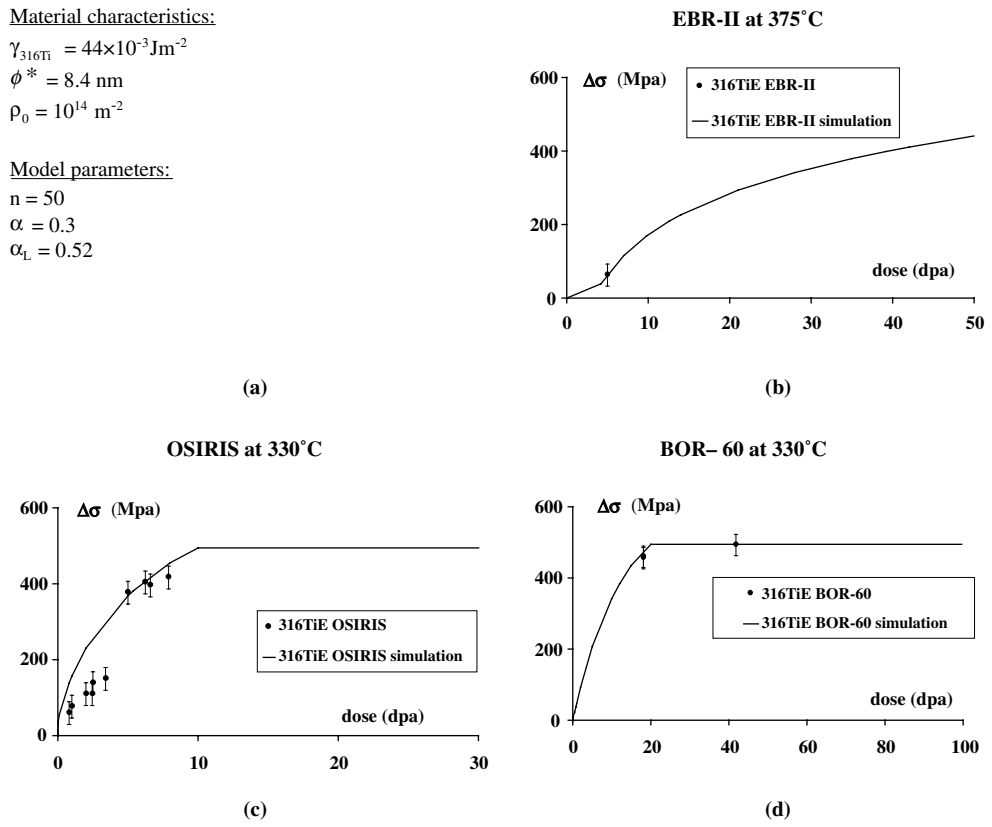

Fig. 7. Evolution of hardening for material CW 316 Ti. (a) Values of material and model parameter, *s* (b) EBR-II, (c) OSIRIS, (d) BOR-60.

$b = 3.12 \times 10^{-10}$ m, $b_f = 2.077 \times 10^{-10}$ m and $b_p = 2.544 \times 10^{-10}$ m. The Taylor factor M is 3.02. The shear modulus $\mu = 82.99$ GPa. γ is taken as a function of the chemical composition [8]:

$$\gamma\ (\mathrm{mJ/m^2}) = 25.7 + 2\ (\%_{\mathrm{Ni}}) + 410\ (\%_{\mathrm{C}}) - 0.9\ (\%_{\mathrm{Cr}}) - 77\ (\%_{\mathrm{N}}) - 13\ (\%_{\mathrm{Si}}) - 1.2\ (\%_{\mathrm{Mn}}).$$

The initial dislocation density ρ_0 has been taken equal to 10^{10} m^{-2} for the solution annealed material, and equal to 10^{14} m^{-2} for the cold worked materials.

The loops diameter and density are calculated by the cluster dynamics model developed in the companion paper which has been shown to describe accurately the experimental data.

The other parameters n, α and α_L have been adjusted in order to describe the experimental data with a reasonable accuracy.

The model is applied using the microstructural results coming from the cluster dynamic model and gives the hardening as a function of the damage dose for each material and each experimental irradiation (Figs. 5–7). The value of n, α and α_L for each case are given in the inserts of Figs. 5–7.

The main relevant differences between the three investigated steels are the initial density of dislocations and the stacking fault energy lower for the 304L steel than respectively for the 316 and 316 Ti steels.

The model describes accurately all the experimental results for irradiation at 330 °C. For the irradiations carried out at 375 °C, the model is accurate predicting the behaviour of work hardened materials, although the prediction for large doses for the CW 316 steel (Fig. 6(b)) needs further experimental validation. For the SA 304 material irradiated at high temperature (375 °C) the model underestimates the actual hardening (Fig. 5(b)). This could be due to the presence of cavities, which were seen for these irradiation conditions only (see paper I) and not taken into account in the present model.

4. Conclusions

A systematic experimental quantitative characterization (mainly microstructural investigation in a

companion paper [1] and yield stress determination in this contribution) has been performed on irradiated SA 304, CW 316 and CW 316Ti austenitic stainless steels for different irradiation conditions in terms of temperatures, fluxes, doses and energy spectra. The evolution of the microstructure in terms of dislocation loops has been simulated with a 'cluster dynamic' model. The description of the microstructure after irradiation was coupled with a Frank loop hardening model giving a quantitative description of the hardening of irradiated austenitic stainless steels.

The hardening is well reproduced by this model; when irradiation damage doses increase, hardening increases; then when loops sizes and densities are large enough for the loops to be defaulted, a saturation of hardening occurs. A criterion of critical density of loops (ρ^* as a function of their size) above which stress induced defaulting will occur has been proposed. According to this model, only the dose from which the hardening saturates (but not the saturation level itself) depends on the irradiation temperature. The saturation level is mainly related to the initial dislocation network and also possibly to the stacking fault energy and to the loop obstacle strength of the material.

The present model is well suited to describe the hardening due to the interstitial loops but the 'cluster dynamic' model fails to describe accurately the vacancy clusters, and notably their transformation into voids. In a steel which can contain dissolved gases, this transformation is favored. Since this phenomenon has been neglected here, one needs to be cautious in the application of the present model to high temperature irradiation.

The defaulting of Frank loops induced by moving dislocations has been recently observed in molecular dynamics simulation [9]. Furthermore this mechanism should lead to local recovery and to localization of plastic deformation evidenced experimentally by the so-called 'channeling' [10]. This is likely to play a major role in the severe loss of ductility observed in irradiated materials.

Acknowledgements

Enlightening discussions with Dr D. Rodney are gratefully acknowledged. Authors are grateful to Dr G.R. Imel at ANL, US, for performing neutron irradiation in EBR-II reactor, Dr V. Golovanov and Professor V. Shamardin at RIAR, Russia for performing neutron irradiations in BOR-60 reactor and to Professor V. Prokhorov for post-irradiation tensile tests. This work was performed in the frame of the French R&D Project 'PWR Internals' sponsored by Electric Power Research Institute (Joint Owner Baffle Bolts Program), Palo Alto, CA, under the responsibility of Dr H.T. Tang whose support is gratefully acknowledged.

References

[1] C. Pokor, Y. Brechet, P. Dubuisson, J.-P. Massoud, A. Barbu, Irradiation damage in 304 and 316 stainless steels: experimental investigation and modeling. Part I: Evolution of the microstructure, this issue. doi:10.1016/j.nucmat.2003.11.007.
[2] J.C. Van Duysen, P. Todeschini, G. Zacharie, 16th International Symposium, ASTM STP 1405, ASTM 2001, p. 413.
[3] J. Friedel, Dislocations, Pergamon, 1964.
[4] D. McLean, Mechanical Properties of Metals, Wiley, New York, 1962, p. 153.
[5] C. Pokor, Caractérisation microstructurale et modélisation du durcissement des aciers austénitiques irradiés des structures internes des réacteurs à eau pressurisée, PhD thesis, Institut National Polytechnique de Grenoble, France, 2002.
[6] D. Rodney, Report CEA-R-5906, 2000.
[7] D. Rodney, G. Martin, Y. Bréchet, Mater. Sci. Eng. A 309–310 (2001) 198.
[8] F.B. Pickering, Proceedings of the Conference on Stainless Steels 84, Göteborg, 3–4 September 1984, p. 2.
[9] C. Pokor, Y. Bréchet, P. Dubuisson, J.P. Massoud, D. Rodney, Irradiation hardening in austenitic steels: experiment and simulation, Osaka, 2003.
[10] M.L. Hamilton, F.H. Huang, W.J.S. Yang, F.A. Garner, in: F.A. Garner, C.H. Henager, N. Igata (Eds.), 13th International Symposium (Part II), ASTM STP 956, American Society for Testing and Materials, Philadelphia, 1987, p. 245.